Journal of ELECTRONIC MATERIALS, Vol. 45, No. 10, 2016
DOI: 10.1007/s11664-016-4722-z

Theoretical Investigation of Mechanical, Electronic, and Thermal Properties of Fe_2TiSi and Fe_2TiSn Under Pressure

JU-YONG JONG,[1,2,3] JINGCHUAN ZHU,[1,4] SU-IL PAK,[2] and GYONG-HO SIM[1]

1.—School of Materials Science and Engineering, Harbin Institute of Technology, Harbin 150001, China. 2.—Department of Energy Science, Kim IL Sung University, Pyongyang, Democratic People's Republic of Korea. 3.—e-mail: jjy429@163.com. 4.—e-mail: zhu-jc@126.com

In this study, the structural, mechanical, electronic, and thermal properties for Fe_2TiSi and Fe_2TiSn Heusler compounds were successfully studied by using the first-principles calculations based on density functional theory for the first time. The lattice constants calculated from the theoretical calculations are consistent with the experimental results, and cell volume decreases uniformly with increasing pressure. The elastic constants and shear moduli, bulk moduli, Young's moduli of these alloys satisfy the traditional mechanical stability restrictions and those are suggesting that ductility of these alloys gradually change for the better with increasing ambient pressure conditions up to the considered pressures. These Heusler materials have small band gaps with flat band at the bottom of the conduction band and the calculated band gaps increase between 0.472 eV and 0.646 eV in Fe_2TiSi, 0.144 eV and 0.175 eV in Fe_2TiSn for pressure ranging from 0 GPa to 50 GPa. Density of states landscapes are considered and predict a better transport properties at a lower pressure. In addition, we predicted the Debye temperatures, the isochoric heat capacities, minimum thermal conductivities of Fe_2TiSn and Fe_2TiSi by using first-principles calculations combined with the quasi-harmonic Debye model under pressure up to 50 GPa.

Key words: Full-Heusler alloy, Fe_2TiSn, Fe_2TiSi, first-principle, pressure, thermoelectric material

INTRODUCTION

Thermoelectric direct conversion, which convert thermal energy to electrical energy, and vice versa, is a very promising avenue for renewable energy generation and solid-state cooling, have attracted attention in various areas such as solar thermal energy conversion, waste heat recovery, and solid state cooling as partial measures for effective use of energy and CO_2 reduction.[1,2] In recent years, several Heusler compounds have attracted great scientific interest due to their possible application because of their high thermoelectric power factor, among which Fe_2VAl is the most prominent example.[3–5] The Fe_2TiSn, Fe_2TiSi compounds, which also belong to the group of Heusler-type alloys are promising candidates to realize a high power factor value, compared to Fe_2VAl.[6,7] Moreover, the Fe_2TiSn, Fe_2TiSi compounds comprise predominantly abundant chemical elements such as Fe, Ti, Sn, Si and contain no toxic elements, hence in terms of abundance and cost of the materials it is very interesting to study these compounds.

Recently, the Heusler compounds Fe_2TiSi, Fe_2TiSn have been predicted to be materials with large Seebeck coefficients (−300 μV/K at room temperature) by using first-principles calculations,[6] and Lue et al. observed that a Seebeck coefficient around 340 K for Fe_2TiSn is compatible with Fe_2VAl (300 K).[8] Markus et al. prepared single phase films of the metastable Fe_2TiSi compound and studied its electronic and transport properties in detail.[9] The

(Received April 11, 2016; accepted June 1, 2016; published online June 15, 2016)

electronic structure and magnetic properties of Fe_2TiSn were studied theoretically,[10–12] and transport and thermoelectric properties including electrical conductivity σ, Seebeck coefficient S, as well as thermal conductivity k in the Heusler-type compound Fe_2TiSn were studied.[8] This was demonstrated, yielding power factors 4–5 times larger than in classical thermoelectrics at room temperature in Fe_2YZ Heusler compounds, using first-principles calculations and the theoretical concept,[7] and Bin Xu et al.'s study on the electronic structure and linear optical properties of the Fe_2TiSn by using the full-potential linearized augmented plane wave and local orbital method.[13]

In application, development, fabrication, and understanding of thermoelectric materials, the elastic, mechanical, electronic, and thermodynamic properties are very important because elastic properties represent the mechanical robustness of the material under pressure, and thermoelectric properties and the phonon transport will be greatly influenced in the presence of structural strain and external pressure, which leads to subtle changes in the thermal conductivity.[14–17]

Li et al. studied on the pressure influence of the band structures of AuX_2 (X = Al, Ga, and In) and found that their transport properties were sensitive to the pressure-tuned band structure close to the Fermi surface.[14] Lanqing et al. suggest possible enhancement of thermoelectric properties for SnTe under intermediate pressure and PbTe[15] under high pressure. Bin Xu et al. studied on the pressure effect of Fe_2VAl thermoelectric material.[16,17] Finally, the pressure effect on the thermoelectric materials is important. However, no data have been reported on the pressure induced structural, mechanical, and thermodynamic properties of Fe_2TiSi and Fe_2TiSn.

In this paper, structural, mechanical, electronic, and thermal properties of Fe_2TiSi and Fe_2TiSn materials at different pressures by using first principles calculations combined with the quasi-harmonic Debye model are measured for the first time.

DETAILS OF CALCULATIONS

The Heusler-type intermetallic compounds Fe_2TiSi, Fe_2TiSn belong to a group of ternary intermetallics X_2YZ with an $L2_1$ structure (space group Fm3m); the lattice consists of four interpenetrating fcc sublattices. The unit cell is an fcc lattice with four atoms of Fe at (0, 0, 0), (1/2, 1/2, 1/2), Ti at (1/4, 1/4, 1/4), and Si or Sn at (3/4, 3/4, 3/4), and each Fe atom has four Ti and four Si or Sn atoms as nearest neighbors, while each Ti and Si or Sn atoms are surrounded by eight Fe atoms. The total energy electronic structure calculations and elastic properties calculations were performed using Cambridge Serial Total Energy Package (CASTEP),[18] based on the density functional theory (DFT) in generalized gradient approximations (GGA) with Perdew–Burke–Ernzerhof (PBE)[19] exchange–correlation potential. Each calculations were considered when the maximum force on the atom was below 0.01 eV/Å, the maximum displacement between cycles was below 5.0×10^{-4} Å, and the energy change was below 5.0×10^{-6} eV/atom. The ultra-soft pseudopotential and plane wave basis sets were used. After a series of tests, the cutoff energy was set at 360 eV. The states of Fe: $3d^64\ s^2$, Ti: $3s^23p^63d^24\ s^2$, Si: $3s^23p^2$, and Sn: $5s^25p^2$ were treated as valence states. In the Brillouin zone integrations, $8 \times 8 \times 8$ k-points were determined according to Monkhorst–Pack scheme[20] and based on the Broyden–Fletcher–Goldfarb–Shenno (BFGS)[21] minimization technique, the system reaches the ground state via self-consistent calculation when the total energy is stable within 5×10^{-7} eV/atom and $<10^{-2}$ eV/Å for the force. Finally, we apply the quasi-harmonic Debye model to investigate the thermal properties of Fe_2TiSi and Fe_2TiSn.

RESULTS AND DISCUSSIONS

In this section, we present the structural, mechanical, electronic, and thermal properties for Fe_2TiSi and Fe_2TiSn Heusler compounds at different pressures and compared with previous theoretical predictions and available experimental data.

Structure Properties

To obtain ground-state properties, the structure was optimized by BFGS method. The optimized ground state lattice parameters, bulk moduli, density of Fe_2TiSi and Fe_2TiSn are listed in Table I. The optimized lattice constants for Fe_2TiSi and Fe_2TiSn are 5.658 Å, 6.033 Å respectively.

The previous experimental and theoretical lattice constants of Fe_2TiSn are 6.074 Å,[22] 6.032 Å,[6] in

Table I. Calculated lattice constants (a), densities (d), formation enthalpies, and bulk moduli (B) of Fe_2TiSn and Fe_2TiSi

	a(Å)		d(g/cm^3)			
Compounds	**This work**	**Exp.**	**This work**	**Exp.**	**ΔH (eV/atom)**	**B (GPa)**
Fe_2TiSi	5.658	5.72[9]	6.87	6.6[9]	−0.64	232.098
Fe_2TiSn	6.032	6.074[22]	8.144		−1.15	189.663

Fe_2TiSi 5.72 Å,[9] 5.685 Å.[6] The lattice parameters are bigger than experimental results, but the differences are $<1\%$, which indicates that the present calculations are highly reliable. If thermodynamic effects on crystal structure calculation are considered, our calculation results should be in good agreement with experimental results, and we can conclude that the computation parameters and conditions selected in this study are suitable. We have also calculated the pressure variations of lattice parameters and plotted in Fig. 1. It can be noted that the volume decreases uniformly with increasing pressure.

The formation enthalpy is defined as the total energy difference between the compound and its constituents in proportion to the composition, the bulk stability of the compound is determined by formation enthalpy. Negative formation enthalpy value implies the structure is thermodynamically stable, while positive value means the structure is unstable. In this work, the formation enthalpy was calculated by the following expression:

$$\Delta H_{Fe_2TiX} = (E_{tot} - 2E^{Fe}_{solid} - E^{Ti}_{solid} - E^{X}_{solid}) \quad (1)$$

where E_{tot} refers to the total energy of unit crystal cell used in the present calculation, E^{Fe}_{solid}, E^{Ti}_{solid}, E^{X}_{solid} are the energy per atom of bulk Fe, Ti, X(Si,Sn). In Table I, calculated formation enthalpies of Fe_2TiSn and Fe_2TiSi at zero pressure are presented, formation enthalpies of Fe_2TiSi and Fe_2TiSn are -0.647 eV/atom, -1.15 eV/atom respectively. The negative heat values of formation of Fe_2TiSi and Fe_2TiSn show that these phases can exist stably.

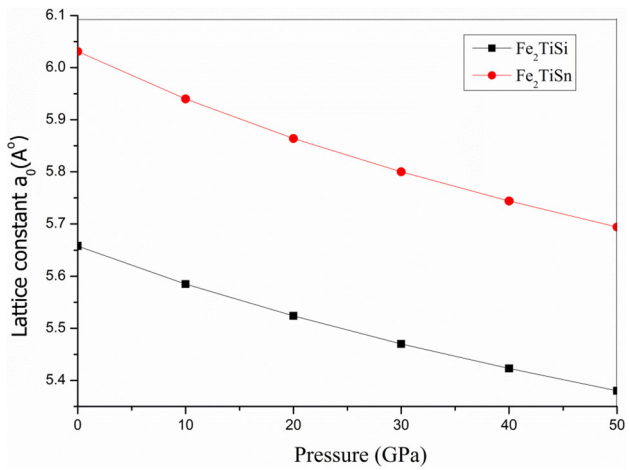

Fig. 1. Pressure induced variations in lattice parameters for Fe_2TiSi and Fe_2TiSn.

Elastic Properties

We analyze the mechanical stabilities of Fe_2TiSi and Fe_2TiSn by calculating their elastic constants. For a cubic crystal, there are three independent stiffness constants, namely C_{11}, C_{12} , and C_{44} by virtue of cubic symmetry, through the calculated elastic constants, we can obtain the information on the stability, ductility, and brittleness of the material. In Table II, the elastic constants of Fe_2TiSi and Fe_2TiSn in the pressure ranging from 0 GPa to 50 GPa are presented, it is noted that C_{ij} increases with the enhancement of pressure. It is clearly seen that elastic constants C_{11}, C_{12}, and C_{44} increase when the pressure is enhanced and those are sensitive to the change of pressure.

From the obtained elastic tensor components, elastic moduli can be derived, such as shear modulus G, bulk modulus B, Young's modulus E by Voigte–Reusse–Hill (VRH) approximations based on G_V (Voigt's shear modulus), and G_R (Reuss's shear modulus);[23] the results are presented in Table III.

The obtained values for all of the investigated systems satisfy the mechanical stability restrictions[24] of $C_{11} > 0$, $C_{44} > 0$, $(C_{11}\text{-}C_{12}) > 0$, and $(C_{11} + 2C_{12}) > 0$, also obey the cubic stability condition: $C_{12} < B < C_{11}$, suggesting their mechanical stabilities. With pressure applied, both B and G are enhanced. B varies 232–467 GPa (Fe_2TiSi), 189–396 GPa (Fe_2TiSn) for pressure ranging from 0 GPa to 50 GPa, and G varies 158–243 GPa (Fe_2TiSi), 116–188 GPa (Fe_2TiSn) within the investigated pressure range.

Generally, Young's modulus of a material is the usual property used to characterize stiffness, the material has higher value of E, is more stiff material. From Table III, the Young's moduli of both materials increase linearly with pressure and Fe_2TiSi is stiffer than Fe_2TiSn.

Table II. Elastic constants C_{ij} of Fe_2TiSn and Fe_2TiSi in the pressure range (0–50 GPa)

	C_{11} (GPa)		C_{12} (GPa)		C_{44} (GPa)	
Pressure (GPa)	**Fe_2TiSi**	**Fe_2TiSn**	**Fe_2TiSi**	**Fe_2TiSn**	**Fe_2TiSi**	**Fe_2TiSn**
0	457	339	119	114	152	118
10	548	407	172	153	171	138
20	600	469	188	193	190	156
30	662	521	223	219	205	181
40	709	575	239	254	223	188
50	802	624	299	283	238	202

Table III. Shear moduli *G*, Bulk moduli *B*, Young's moduli *E*, *B*/*G* ratios of Fe_2TiSi and Fe_2TiSn at different pressures

	G (GPa)		*B* (GPa)		*E* (GPa)		*B*/*G*	
P (GPa)	Fe_2TiSi	Fe_2TiSn	Fe_2TiSi	Fe_2TiSn	Fe_2TiSi	Fe_2TiSn	Fe_2TiSi	Fe_2TiSn
0	158.7	116	232.1	189.7	387.7	289.1	1.463	1.635
10	178	133.9	297.8	238	445.3	338.3	1.673	1.777
20	196.9	148.8	325.6	285.6	491.5	380.4	1.654	1.919
30	210.7	168.7	370.1	319.9	531.4	430.5	1.756	1.896
40	228.1	176.8	395.9	361.8	574	456	1.736	2.047
50	243.5	188.7	467.1	396.9	622.3	488.6	1.918	2.104

The other experimental and theoretical values of elastic constants for Fe_2TiSn and Fe_2TiSi are not available yet. However, by comparing with earlier reported E(283.58 GPa), B(197.81 GPa), G(112.44 GPa) calculations based on GGA for similar compound Fe_2TiAl at zero pressure,[25] we believe that our predicted properties for Fe_2TiSn and Fe_2TiSn are reasonable and can be used as references for the experiments or theories. Furthermore, ratio of the bulk modulus to shear modulus of crystalline phases can also predict the brittle and ductile behavior of materials. Higher (lower) B/G ratio corresponds to ductile (brittle) behavior, the critical value which separates ductile and brittle materials is around 1.75. The data in the Table III shows that the B/G ratios vary between 1.46 and 1.91(Fe_2TiSi), 1.63 and 2.1(Fe_2TiSn) for pressure ranging from 0 to 50 GPa, suggesting that ductility of these alloys gradually change for the better with increasing ambient pressure. These calculations suggest that Fe_2TiSi and Fe_2TiSn may withstand pressure without substantial structural damage; therefore, their physical properties should be evaluated under pressure.

Electronic Properties

Usually, the figure of the band structure near the Fermi level determine the thermoelectric properties of a material and band gap is very useful in obtaining reliable transport properties in thermoelectric materials. It has been studied previously that the value of band gap can influence the thermoelectric performance significantly under the normal working conditions, accurate band gap is very important in the transport analysis.[26]

In order to investigate band variations theoretically, the band structure calculations of Fe_2TiSn and Fe_2TiSi by CASTEP package were performed in a pressure range of 0–50 GPa. The band structure details are exhibited as follows (Fig. 2).

Fe_2TiSi and Fe_2TiSn are semiconductors with flat band at the bottom of the conduction band along the *G*–*X* directions. The valence band maximum and conduction band minimum (at the *G* point) mainly consist of Fe 3d (t_{2g}) orbitals and Fe 3d (e.g.) orbitals, respectively. These band structures are well consistent with previous literature.[6,9] The obtained band gaps are 0.144 eV for Fe_2TiSn and 0.472 eV for Fe_2TiSi at 0 GPa. Shin et al. studied temperature dependence of the thermoelectric properties of these compounds at different band gaps,[6] our calculated results imply that these materials could be good thermoelectric materials at room temperature. Because DFT functionals are usually known to underestimate band gaps, this calculated

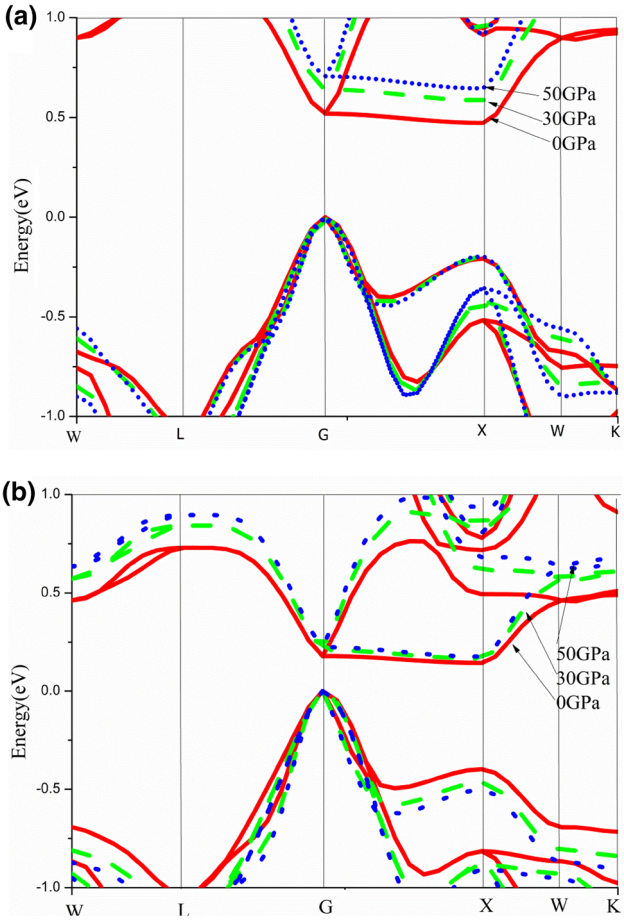

Fig. 2. Band structure of (a) Fe_2TiSi and (b) Fe_2TiSn versus pressure.

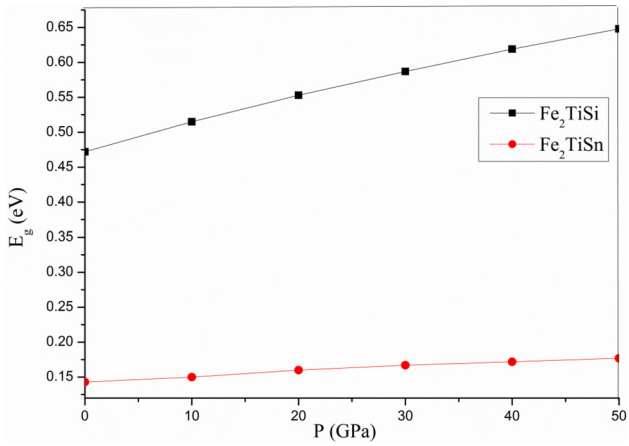

Fig. 3. Variation of band gaps of Fe_2TiSi and Fe_2TiSn versus pressure.

value in DFT framework may be slightly underestimated compared with experimental values; unfortunately, there are no reports on experimental band gap values of Fe_2TiSn and Fe_2TiSi.

Figure 3 illustrates the obtained band gaps under various pressures. Both compounds have small band gaps, and the calculated band gaps vary between 0.472 eV and 0.646 eV in Fe_2TiSi, 0.144 eV and 0.175 eV in Fe_2TiSn for pressure ranging from 0 GPa to 50 GPa. Band gap variation of the Fe_2TiSn under the effect of pressure is smaller than band gap change of the Fe_2TiSi by the application of the pressure.

It was calculated the density of states (DOS) upon pressure for more understanding electronic properties. The total and partial densities of states (TDOS and PDOS) at different pressures for Fe_2TiSn and Fe_2TiSi are calculated and plotted in Fig. 4. The main contributions to the DOS near the Fermi level of these materials come from the d orbitals of Fe. From the Fe-PDOS, the state distributions are broadened and the conduction bands are shifted away from the Fermi level as the pressure increased. The valence bands do not express significant movement; however, the energy states also accumulate near the Fermi level when the pressure decreases.

From Fig. 4, we can further see that the PDOS of Fe exhibit sharper increase near the Fermi level when the pressure is lower. Since dense energy states and large derivates near Fermi level are generally related with improved transport properties such as high Seebeck coefficients, we can expect enhanced thermoelectric performance within these materials under low pressure. But the overall shape of DOS and PDOS of Fe_2TiSi and Fe_2TiSn change slightly when under high pressure, which means the pressure only has no so large effect on electronic properties of these alloys.

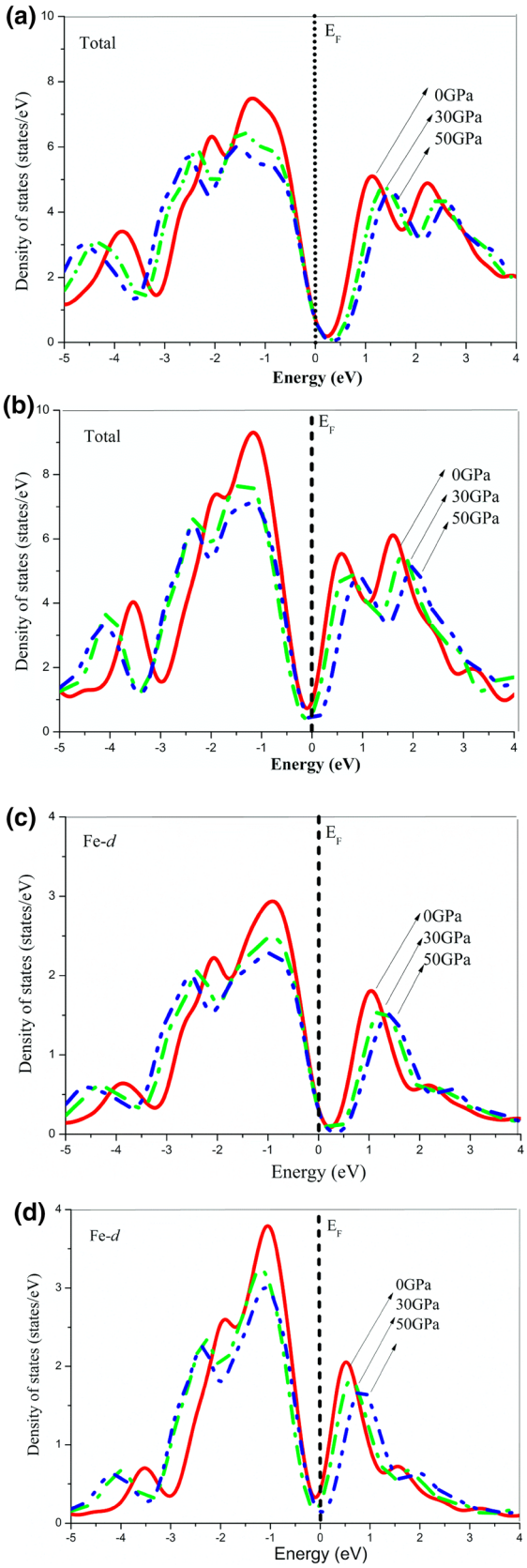

Fig. 4. Total densities of states (a) Fe_2TiSi, (b) Fe_2TiSn and partial densities of states (c) Fe_2TiSi, (d) Fe_2TiSn.

Table IV. Calculated transverse (v_t), longitudinal (v_l), and mean sound speeds (v_m) and thermal conductivity (κ_{min}) for Fe_2TiSi and Fe_2TiSn at different pressures

	v_l (m/s)		v_t (m/s)		v_m (m/s)		κ_{min} (W m^{-1} K^{-1})	
P (GPa)	Fe_2TiSi	Fe_2TiSn	Fe_2TiSi	Fe_2TiSn	Fe_2TiSi	Fe_2TiSn	Fe_2TiSi	Fe_2TiSn
0	8031.4	6397.2	4803.2	3713.2	5315.2	4120.4	1.46	0.99
10	8650.9	6874.3	4989.5	3897.8	5539.8	4334	1.56	1.08
20	8920.2	7269.7	5160.9	4031	5728.5	4490.2	1.65	1.14
30	9249.3	7585.2	5262.3	4220.9	5849.6	4700.4	1.71	1.22
40	9466.3	7828	5403.5	4258	6004.8	4750	1.79	1.26
50	9948.4	8048.7	5516.9	4341.5	6145.4	4846.2	1.86	1.31

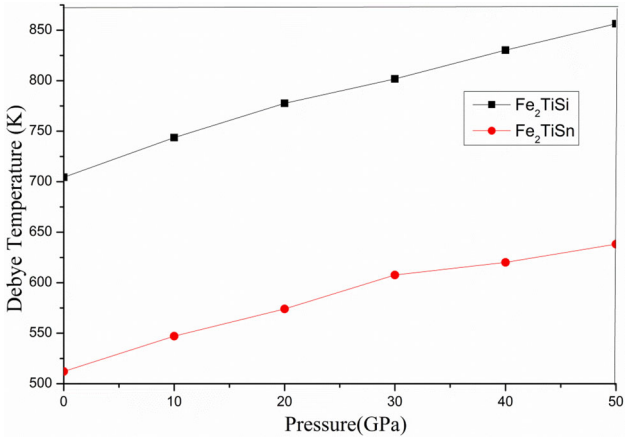

Fig. 5. Variations of the Debye temperatures for Fe_2TiSn and Fe_2TiSn for pressure ranging from 0 GPa to 50 GPa.

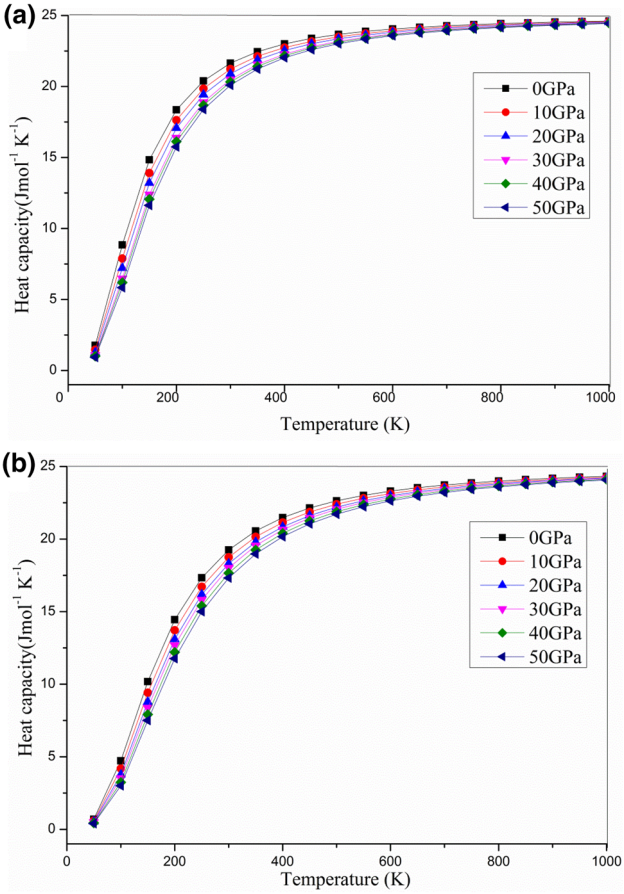

Fig. 6. Heat capacities of (a) Fe_2TiSi and (b) Fe_2TiSn versus pressure at various temperatures.

Thermal Properties

The Debye temperature (Θ_D) is known to be an important fundamental parameter closely related to many physical properties, such as specific heat and melting temperature. Furthermore thermal properties are very important in the thermoelectric materials. At low temperatures, the vibration excitations generate totally from acoustic vibrations. Hence, the Debye temperature calculated from elastic properties is the same as that determined from specific heat measurements, one method to obtain the Θ_D values of materials is from elastic constants.[27–29]

We have calculated the Debye temperatures (Θ_D) for Fe_2TiSi and Fe_2TiSi under pressure by

$$\theta_D = \frac{h v_m}{k_B}\left[\frac{3n\rho N_A}{4\pi M}\right]^{\frac{1}{3}} \quad (2)$$

where h is Planck's constant, and k_B Boltzmann's constant, N_A Avogadro's number, ρ the density of material, M the molecular weight, and n the number of atoms per formula unit. v_m is the mean sound velocity, it can be calculated from v_l (longitudinal elastic wave velocity) and v_t (transverse elastic wave velocity), which can be calculated by using the bulk modulus (B) and the shear modulus (G) from Navier's equation.[28]

The calculated values of v_m, v_l, v_t for Fe_2TiSn and Fe_2TiSn compounds at different pressures are given in Table IV. Figure 5 shows the variations of the Debye temperatures of these alloys for pressures ranging from 0 GPa to 50 GPa.

Accordingly, the increase of ambient pressure leads to an increase of Debye temperatures and mean sound velocities v_m in the Fe_2TiSi and

Fe_2TiSn. As far as we know, there are also no experimental and theoretical data on these alloys available in the literature for a meaningful comparison. Then, the isovolumic heat capacity C_v was calculated from Debye model. Figure 6 shows the calculated C_v of Fe_2TiSi and Fe_2TiSn in the temperature range from 0 K to 1000 K at different pressure. In these materials, the calculated C_v will approach the limiting Dulong–Petit value of $3R$ (24.94 J mol^{-1} K^{-1}) at high temperatures.

It can be seen from Fig. 6 that the heat capacity increases with the temperatures at the same pressure and decreases with the pressures at the same temperature. The influences of the temperature on the heat capacity are much more significant than that of the pressure on it.

The thermal conductivity is the important property of a thermoelectric material that indicates its ability to conduct heat. Thus, in order to know if material is a candidate for thermoelectric application, its thermal conductivity needs to be investigated. It is difficult to estimate the lattice thermal conductivity at a high temperature using first-principles calculations. However, the minimum thermal conductivity can be calculated under the assumption that the lattice thermal conductivity in glasses and complex crystals may approach κ_{min} at relatively low temperature, compared with the melting temperature at which the κ_{min} is reached for simple crystal structures.[29] Clarke[30] suggested that the theoretical minimum thermal conductivity κ_{min} can be calculated after replacing different atoms by an equivalent atom with a mean relative atomic mass. The formulas are given by

$$\kappa_{min} = 0.87 k_B \left(\frac{M_m}{n d N_A}\right)^{-\frac{2}{3}} \left(\frac{E}{d}\right)^{\frac{1}{2}} \quad (3)$$

where n, M_m, N_A, E, d, and k_B are the number of atoms in the crystal, molecular weight, Avogadro's constant, Young's modulus, density, and Boltzmann's constant, respectively. The density of Fe_2TiSn and Fe_2TiSi are present in Table I. Using Clark's model, the minimum thermal conductivities (κ_{min}) of these materials were calculated at different pressures (presented in Table IV), κ_{min} of Fe_2TiSn and Fe_2TiSi increase with increasing ambient pressure

Unfortunately, until now, there are no data available related to these properties in the literature for Fe_2TiSn and Fe_2TiSi. Therefore, our calculated values can be considered prediction of these properties. Future experimental work will provide a comparison for our calculated results.

CONCLUSION

In this study, the structural, mechanical, electronic, and thermal properties for Fe_2TiSi and Fe_2TiSn Heusler compounds were successfully studied by using the first principles calculations based on the density functional theory at different pressures.

(1) Noted that as the volume decreases uniformly with increasing pressure, calculated formation enthalpies of Fe_2TiSn and Fe_2TiSi at zero pressure are −0.647 eV/atom and −1.15 eV/atom, respectively.
(2) The elastic constants and shear moduli G, bulk moduli B, Young's moduli E of Fe_2TiSn and Fe_2TiSi satisfy the traditional mechanical stability restrictions and those suggest that ductility of these alloys gradually changes for the better with increasing ambient pressure conditions up to the considered pressures (0 GPa–50 GPa).
(3) Fe_2TiSn and Fe_2TiSi have small band gaps with flat band at the bottom of the conduction band, and the calculated band gaps increase between 0.472 eV and 0.646 eV in Fe_2TiSi, 0.144 eV and 0.175 eV in Fe_2TiSn for pressure ranging from 0 GPa to 50 GPa, which implies that it is potentially good thermoelectric material.
(4) Density of states landscapes of Fe_2TiSn and Fe_2TiSi demonstrate state distributions are broadened and the conduction bands are shifted away from the Fermi level as the pressure increased, which is illustrated a higher Seebeck coefficients at a lower pressure. But high pressure effect on its electronic properties is not so large.
(5) We predicted the Debye temperatures (Θ_D), the isochoric heat capacities(C_V), minimum thermal conductivities (κ_{min}) of Fe_2TiSn and Fe_2TiSi under pressure up to 50 GPa.

ACKNOWLEDGEMENTS

This work was supported by the National Natural Science Foundation of China (Grant No. 51401099).

REFERENCES

1. L.E. Bell, *Science* 321, 1457 (2008).
2. T.M. Tritt, H. Böttner, and L.D. Chen, *MRS Bull.* 33, 366 (2008).
3. Y. Nishino, S. Deguchi, and U. Mizutani, *Phys. Rev. B* 74, 115115 (2006).
4. M. Mikami, K. Kobayashi, T. Kawada, K. Kubo, and N. Uchiyama, *Jpn. J. Appl. Phys.* 47, 1512 (2008).
5. M. Mikami and M. Mizoshiri, *J. Electron. Mater.* 43, 1922 (2014).
6. Y. Shin, O. Masakuni, N. Akinori, Y. Kurosaki, and J. Hayakawa, *Appl. Phys. Express* 6, 025504 (2013).
7. D.I. Bilc, H. Geoffroy, W. David, G.M. Rignanese, and P. Ghosez, *Phys. Rev. Lett.* 114, 136601 (2015).
8. C.S. Lue and Y.K. Kuo, *J. Appl. Phys.* 96, 2681 (2004).
9. M. Meinert, M.P. Geisler, J. Schmalhorst, U. Heinzmann, E. Arenholz, W. Hetaba, M. Stöger-Pollach, A. Hütten, and G. Reiss, *Phys. Rev. B* 90, 085127 (2014).
10. A. Jezierski and A. Slebarski, *J. Magn. Magn. Mater.* 223, 33 (2001).
11. A. Ślebarski, M.B. Maple, and E.J. Freeman, *Phys. Rev. B* 62, 3296 (2000).

12. S.V. Dordevic and D.N. Basov, *Phys. Rev. B* 66, 075122 (2002).
13. B. Xu and L. Yi, *J. Phys. D Appl. Phys.* 41, 095404 (2008).
14. Q. Li, Y. Li, T. Cui, Y. Wang, L. Zhang, Y. Xie, Y. Niu, Y. Ma, and G. Zou, *J. Phys.* 19, 425224 (2007).
15. L. Xu, H. Wang, and J. Zheng, *J. Electron. Mater.* 40, 641 (2011).
16. B. Xu and X. Li, *J. Alloy. Compd.* 565, 22 (2013).
17. T. Naka and T. Adschiri, *J. Magn. Magn. Mater.* 310, 1059 (2007).
18. M.D. Segall, M.D. Segall, P.J.D. Lindan, M.J. Probert, C.J. Pickard, P.J. Hasnip, S.J. Clark, and M.C.J. Payne, *J. Phys.* 14, 2717 (2002).
19. J.P. Perdew, K. Burke, and M. Ernzerhof, *Phys. Rev. Lett.* 77, 3865 (1996).
20. H.J. Monkhorst and J.D. Pack, *Phys. Rev. B* 13, 5188 (1976).
21. H. Fischer and J. Almlof, *J. Phys. Chem.* 96, 9768 (1992).
22. A. Ślebarski, *J. Phys.* 39, 856 (2006).
23. R. Hill, *Phys. Soc. Sect. A* 65, 349 (1952).
24. Z.J. Wu, E.J. Zhao, H.P. Xiang, X.F. Hao, X.J. Liu, and J. Meng, *Phys. Rev. B.* 76, 054115 (2007).
25. V. Sharma and G. Pilania, *J. Magn. Magn. Mater.* 339, 142 (2013).
26. L. Xu, Y. Zheng, and J. Zheng, *Phys. Rev. B* 82, 195102 (2010).
27. O.L. Anderson, *J. Phys. Chem. Solids* 24, 909 (1963).
28. P. Wachter, M. Filzmoser, and J. Rebizant, *Phys. B* 293, 199 (2001).
29. L.B. Guo, Y.X. Wang, Y.L. Yan, G. Yang, J.M. Yang, and Z.Z. Feng, *J. Appl. Phys.* 116, 033705 (2014).
30. D.R. Clarke, *Surf. Coat. Technol.* 163, 67 (2003).